Heteroepitaxial structures of $SrTiO_3$/TiN on Si(100) by *in situ* pulsed laser deposition

R. D. Vispute, J. Narayan, K. Dovidenko, and K. Jagannadham
Department of Materials Science and Engineering, North Carolina State University, Raleigh, North Carolina 27695-7916

N. Parikh and A. Suvkhanov
Department of Physics and Astronomy, University of North Carolina, Chapel Hill, North Carolina 27599

J. D. Budai
Solid State Division, Oak Ridge National Laboratory, Oak Ridge, Tennessee 37831

(Received 21 March 1996; accepted for publication 18 September 1996)

High-quality ceramics based heteroepitaxial structures of oxide-nitride-semiconductors, i.e., $SrTiO_3$/TiN/Si(100) have been fabricated by *in situ* pulsed laser deposition. The dependence of substrate temperature and oxygen partial pressure on the crystalline quality of the $SrTiO_3$ films on Si with epitaxial TiN template has been examined. We found that epitaxial growth occurs on TiN/Si(100) above 500 °C, initially at a reduced O_2 pressure (10^{-6} Torr), and followed by a deposition in the range of $5-10\times10^{-4}$ Torr. X-ray diffraction (Θ, ω, and Φ scans) and transmission electron microscope (TEM) results revealed an excellent alignment of $SrTiO_3$ and TiN films on Si(100) with a cube-on-cube epitaxy. Rutherford backscattering and ion channeling results show a channeling minimum yield ($\chi_{\min}$) of ~13% for the $SrTiO_3$ films. High-resolution TEM results on the $SrTiO_3$/TiN interface show that the epitaxial $SrTiO_3$ film is separated from the TiN by an uniform 80–90 Å crystalline interposing layer presumably of TiN_xO_{1-x} (oxy-nitride). The $SrTiO_3$ film fabricated at 700 °C showed a high relative dielectric constant of 312 at the frequency of 1 MHz. The electrical resistivity and the breakdown field of the $SrTiO_3$ films were more than 5×10^{12} Ω cm and 6×10^5 V cm^{-1}, respectively. An estimated leakage current density measured at an electric field of 5×10^5 V/cm^{-1} was less than 10^{-7} A/cm^2. © *1996 American Institute of Physics.* [S0021-8979(96)09224-9]

I. INTRODUCTION

With the increase of device number density in dynamic random access memories (DRAMs), the charge-storage limit of Si-based dielectrics (oxides and nitrides) in capacitor cells is being rapidly approached with each new generation of device structures.[1] This has revived the search for new dielectrics with higher permittivity and charge storage capabilities.[2] One class of very attractive materials is the family of crystalline perovskites.[2,3] Since the grain boundaries induce high leakage current and amorphous layers have a low dielectric constant, heteroepitaxial growth of perovskites on semiconductors such as Si is immensely important because they have outstanding properties that can be exploited for the future development of microelectronics and optoelectronics.[4–7] In this article, we report epitaxial growth of $SrTiO_3$ (STO) films on Si(100) using TiN as a template layer. The epitaxial growth of STO on metallic TiN is not only interesting in the context of epitaxy (oxide on nitride), but also for future development of 3D heterostructures on Si based on their potential applications for new generation of microelectronics and superconducting devices. It should be mentioned that in the previous studies the STO films deposited on Si substrates were found to be either polycrystalline/textured or poorly aligned with extensive interdiffusion at the interface,[8] which severely limited the usefulness of these structures. In the present case, epitaxially grown cubic-TiN template on Si promotes high degree of epitaxy for STO, and also provides sharp interfaces without oxidation of the Si surface. The other advantages of epitaxial TiN include: (i) an electrical contact for devices (epitaxial TiN is a desirable conducting layer with electrical resistivity as low as 15 $\mu\Omega$ cm at room temperature for contact metallization, and a diffusion barrier in silicon technology),[9,10] and (ii) the domain matching epitaxial growth[9,10] eliminates grain boundaries and fast dopant diffusion along grain boundaries. Besides the advantages of bottom contact layer, TiN has excellent structural, chemical and thermal compatibility with STO and Si as compared to Pt,[4] Sr,[5] Ti,[5] $SrVO_3$,[5] SrF_2,[5] CaF_2[6] buffer layers investigated previously.

II. EXPERIMENT

The experimental details of our pulsed laser deposition (PLD) are described elsewhere.[9,10] Briefly, a KrF excimer laser was used to ablate stoichiometric, hot pressed TiN target at an energy density of 10 J cm^{-2}, and a single-crystal STO target at 3 J cm^{-2}. Before deposition, the Si(100) substrates were cleaned using 5% HF solution. In the case of STO depositions, films were grown at different substrate temperature (T_s) ranging from 400 to 750 °C, initially at a reduced O_2 partial pressure ~10^{-6} Torr, and then followed by a deposition at a high pressure ranging from 10^{-5} to 10×10^{-4} Torr, pulse repetition rate of 10 Hz for 7–10 min. The typical average growth rates of STO films achieved in our experiments with the use of an energy density of 3 J/cm^2 and oxygen partial pressure of 5×10^{-4} Torr are in the range of 0.7–0.8 Å per pulse. These heterostructures were charac-

Downloaded¬15¬Nov¬2002¬to¬129.2.41.143.¬Redistribution¬subject¬to¬AIP¬license¬or¬copyright,¬see¬http://ojps.aip.org/japo/japcr.jsp

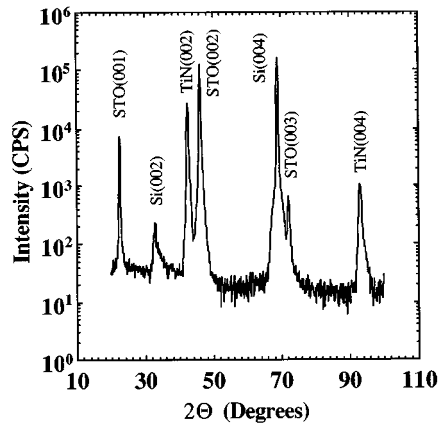

FIG. 1. XRD pattern of the epitaxial STO film grown on TiN/Si(100) at 700 °C and O_2 pressure of 5×10^{-4} Torr.

TABLE I. The FWHM of ω-rocking curves measured on STO(002) reflection, and RBS channeling of STO films grown on epitaxial TiN/Si(100) at various substrate temperatures. For comparative studies, the FWHM for TiN and STO films grown on Si(100) are also presented.

Heterostructure	Substrate temperature	FWHM of ω-curve	RBS χ_{min}
STO/Si(100)	700°	2.4°	⋯
TiN/Si(100)	600°	0.7°	10%
STO/TiN/Si(100)	400°	3.2°	⋯
STO/TiN/Si(100)	500°	1.8°	⋯
STO/TiN/Si(100)	600°	1.0°	15%
STO/TiN/Si(100)	700°	0.8°	13%
STO/TiN/Si(100)	750°	1.2°	17%

terized by high-resolution x-ray diffraction (XRD) (Θ, ω, and Φ scans), and Rutherford backscattering (RBS) and channeling techniques. The nature and the quality of epitaxy in these films were studied using high-resolution transmission electron microscope (TEM) with point-to-point resolution of 1.8 Å. The surface morphology and film uniformity were investigated by using scanning electron microscopy (SEM). The film thickness and the film uniformity were also verified by using alpha-step 200-Tencor Instruments. The electrical properties of the STO films were investigated in metal-insulator-metal type capacitor structures. The capacitance-voltage ($C-V$) and current-voltage ($I-V$) characteristics were obtained by using the Boonton capacitance meter and HP4145A Device tester, respectively.

III. RESULTS AND DISCUSSION

In this study, epitaxial TiN templates (~1000 Å) were deposited at optimized conditions such as T_s of 600 °C and base pressure of 5×10^{-7} Torr.[9,10] The XRD and TEM results showed that the TiN films were single crystal in nature with cube-on-cube epitaxial relationship. The best full width at half maximum (FWHM) of the ω-rocking curve for the TiN(002) was 0.7°, while the FWHM of Si(004) peak was 0.1°. The RBS channeling yield for these films was found to be in the range of 10–13%. The TiN/Si interface was found to be quite sharp without any indication of interfacial reaction. Four-point-probe electrical resistivity measurements showed characteristic metallic behavior with the lowest resistivity of ~15 $\mu\Omega$ cm at 20 °C. These optimized processing parameters were used to maintain the quality of the template layers for *in situ* fabrication of STO/TiN/Si(100) heterostructures.

The critical parameters for epitaxy of STO on TiN/Si are T_s and O_2 partial pressure during thin-film growth. The STO grows epitaxially at T_s as low as 500 °C with a small contribution of (110) misoriented grains and the crystalline quality of the films improves with increase of T_s up to 700 °C. The O_2 partial pressure significantly affects the structural stability of the heterostructures. In the low-pressure regime, films grown in a base pressure of 10^{-6} Torr were oxygen deficient.[11] In the high pressure regimes, i.e., more than 1 mTorr, the oxidation of TiN layer occurred, and due to the structural transformation of TiN (cubic to rutile) into poly-TiO_2, the top STO film exhibited strain that led to cracking of the films. The stable heterostructures with good crystalline quality were fabricated in O_2 partial pressures of 5×10^{-4} Torr. In this pressure regime, molecular-beam-epitaxy-like condition can also be obtained in PLD as noted for growth of STO on MgO(100) by Hiratani *et al.*[11] and a large migration energy is retained on the substrate surface as compared to deposition at higher O_2 pressures. Figure 1 shows XRD ''$\Theta-2\Theta$'' angular scans of the STO film on TiN/Si(100) at T_s of 700 °C and oxygen partial pressure of 5×10^{-4} Torr. The diffraction pattern shows only {001} family of planes of STO and TiN indicating that the films are highly oriented/textured along the film normal. The x-ray rocking curve was obtained to investigate the film alignment with respect to the substrate normal. The full width at half maximum (FWHM) was used as a measure of the crystalline quality of the films. The rocking curve width and hence epitaxial growth of STO was found to be a strong function of T_s (Table I). The narrowest rocking curve obtained for STO films, grown on TiN/Si(100) at 700 °C was 0.8°, indicating a good alignment of (001) lattice planes with that of TiN(001) and Si(001). This value is significantly lower than that of the previously reported STO/X/Si(100) (X=Sr, Ti, $SrVO_3$, CaF_2, SrF_2),[5,6] wherein FWHM was in the range of 1.8–3.5°.[4–6] The characteristics of in-plane epitaxy were obtained using Φ scans of 1500 Å STO film grown on TiN/Si(100) at 700 °C and oxygen partial pressure of 5×10^{-4} Torr, and the results are shown in Fig. 2. Peak occurring at every 90° corresponds to a good alignment of the a and b axes of the STO and TiN films with Si(100) substrate for cube-on-cube orientation, i.e., the crystallography of the heterostructures was revealed to be STO[100]‖TiN[100] and STO[010]‖TiN[010]. No misoriented in-plane material was observed. The peak widths in phi scans of the STO and TiN were ~2.0° and 2.2°, respectively. The resolution in Φ scan as measured on Si(202) peak was ~0.5°. It is interesting to note that the in-plane alignement of STO film on TiN/Si is quite different than that in Ref. 5, which reported 45° rotation of STO unit cell on Si[100] with lattice misfit of 1.7%. In spite of large lattice misfits between STO-TiN and TiN-Si

Downloaded¬15¬Nov¬2002¬to¬129.2.41.143.¬Redistribution¬subject¬to¬AIP¬license¬or¬copyright,¬see¬http://ojps.aip.org/japo/japcr.jsp

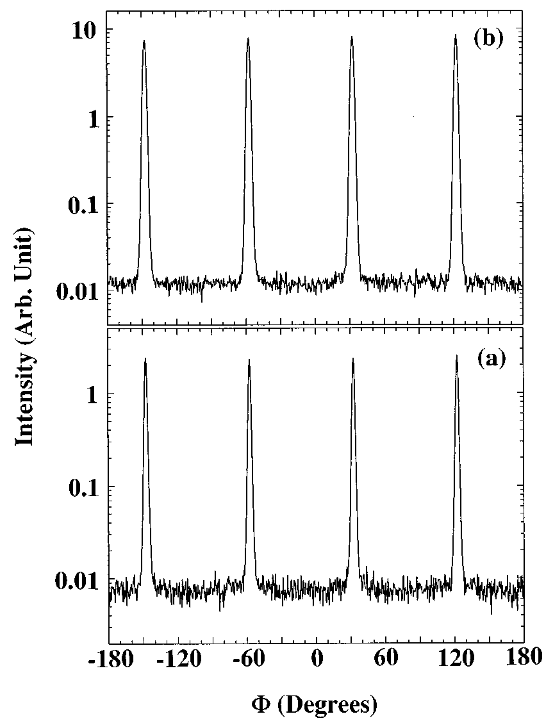

FIG. 2. X-ray diffraction Φ scans of STO/TiN/Si(100) heterostructure, (a) TiN(202) and (b) STO(202) family reflections with the rotation axis normal to the plane of the substrate.

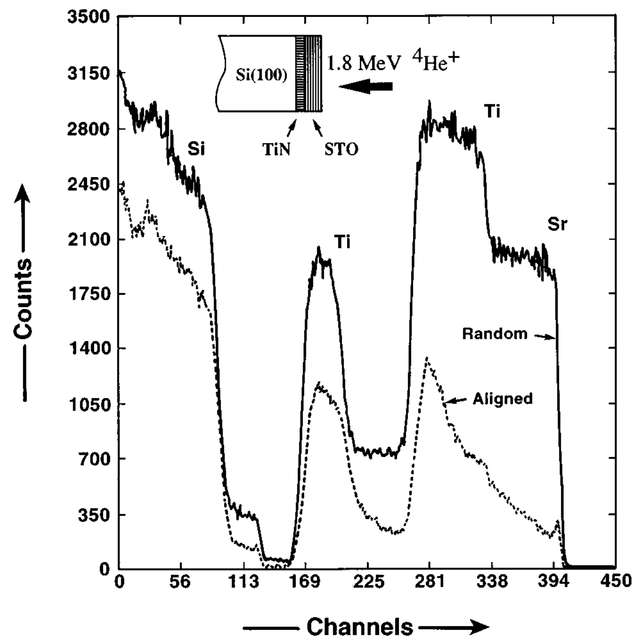

FIG. 3. Random and aligned Rutherford backscattering spectra of the epitaxial STO/TiN/Si(100) heterostructure.

($\sim$8% and 15%, respectively), we did not observe any 45° rotation in the film with respect to the substrate. This suggests that the crystal structure, chemical nature and interfacial energy between the film and the template are the most important parameters which determine the orientation and epitaxy of the film.

The crystalline quality of STO films grown at various T_s was also characterized by an ion channeling using 1.8 MeV $^4He^+$ ions (Table I). Figure 3 shows aligned and random backscattering spectra for a STO film grown on TiN/Si(100) at 700 °C and O_2 partial pressure of 5×10^{-4} Torr. The ratio of the backscattered yield along [001] to that in a random direction (χ_{min}) for Sr, which reflects on the crystalline quality of the STO film, is 13%. This indicates excellent crystallinity of the STO film on TiN/Si(100). This value is significantly better than that of previously published values for STO films grown on Si.[5] However, χ_{min} increases towards the STO/TiN interface indicating channeling discontinuity near the interface. The enhanced scattering near the STO/TiN interface is indicative of higher defect density (disorder in atomic planes).[5,12,13] The RBS spectrum in random direction for the STO in STO/TiN/Si(100) heterostructure can also be well fitted by a computer simulation with the stoichiometric ratio close to that of a bulk target.

The nature of epitaxial growth and interfacial microstructures were also studied using high-resolution electron microscopy. A selected area electron diffraction pattern of a STO/TiN/Si sample fabricated at 700 °C and O_2 pressure of 5×10^{-4} Torr, also confirms a single-crystal nature of the films with cube-on-cube epitaxy which is consistent with XRD and RBS results. Figure 4 shows the HRTEM lattice image of the STO/TiN interface. At the interface, we found that {111} TiN lattice planes are aligned with the {111} STO in addition to an interposing crystalline layer of 80–90 Å thickness. We envisage that the formation of this thin crystalline layer is due to a slow diffusion of oxygen from STO into TiN resulting in an oxy-nitride layer. In the context of epitaxy, the lattice misfit between STO-TiN, and TiN-Si are 8% and 15%, respectively. The epitaxial growth in the large lattice-mismatched systems has been discussed in terms of domain matching epitaxy (DME) in our previous reports,[8,9,11] where integral multiple of major lattice planes match across the film-substrate interface. The epitaxial growth of STO on TiN can be explained on the basis of crystallography and the crystal chemistry. We assume that during STO growth, the TiN surface (top monolayer) is oxidized and forms a Ti-O_2 plane identical to that of Ti-O_2 plane in STO except the higher Ti–O bond length (close to that of Ti–N which is 3.05 Å). The dislocations are gener-

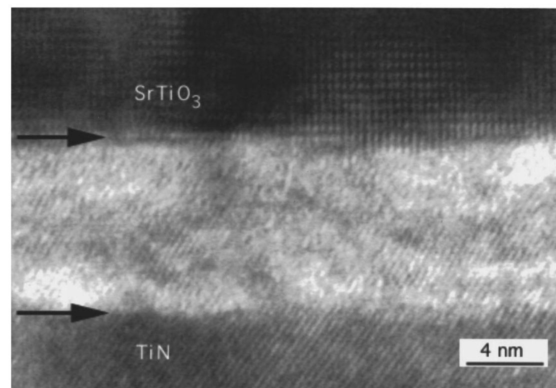

FIG. 4. HRTEM micrograph from STO/TiN/Si heterostructure fabricated at 700 °C and O_2 pressure of 5×10^{-4} Torr.

Downloaded¬15¬Nov¬2002¬to¬129.2.41.143.¬Redistribution¬subject¬to¬AIP¬license¬or¬copyright,¬see¬http://ojps.aip.org/japo/japcr.jsp

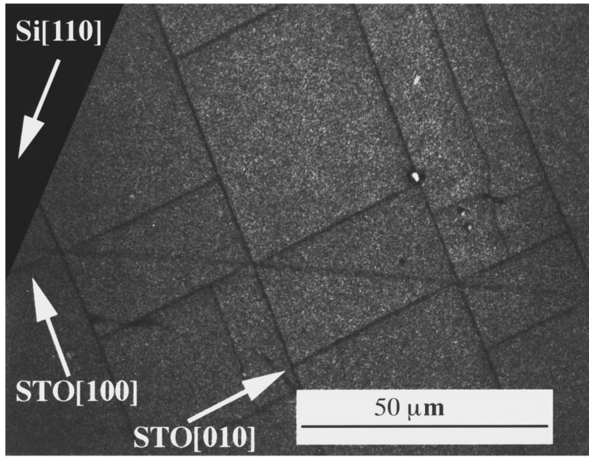

FIG. 5. Optical micrograph of ~5500 Å epitaxial STO film grown on TiN/Si(100) showing relaxation of the films by cracking along [100] and [010] directions. The cleavage planes for Si and STO are {110} and {100}, respectively.

ated and the strain layer is then relaxed by gradually changing the Ti-O distance (close to that of Ti-O in STO which is 2.84 Å) and the growth of single-crystal STO begins subsequently.

The surface morphology of a 1800 Å epitaxial STO films on TiN/Si(100) was found to be very smooth with a low density of particulate ($\sim 1\times10^4$ cm^{-2}) which are often observed in the PLD films. However, for thicker films (~5500 Å), cracks were observed along [100] and [010] directions as shown in Fig. 5. Due to thermal induced strains in the STO films. The thermal strains ϵ_{ab} in TiN and STO were found to be 0.51% and 0.58% for TiN and STO, respectively. The crack propagation along cleavage planes indicates that the STO film is essentially a single crystal.

The dielectric properties of STO films with bottom TiN electrode were investigated from $I-V$ and $C-V$ characteristics of MIMS (metal-insulator-metal-semiconductor) structures. The several gold top electrodes of size varying from 0.5 to 0.8 mm in diameter were sputtered through metal mask to form MIM capacitors. Figure 6 shows the current density versus applied voltage characteristics at room temperature for a 1800-Å-thick STO film deposited on TiN/Si at 700 °C, and O_2 pressure of 5×10^{-4} Torr. The leakage current density was found to be $\sim 10^{-7}$ A cm^{-2} at an electric field of 5×10^5 V cm^{-1}. At higher fields, the electrical conduction was dominated by space-charge controlled conduction process. This type of conduction process has also been observed by Krupanidhi *et al.*[3,4] in their STO films prepared by PLD. The resistivity of the STO films deposited at 700 °C was $\sim 5\times10^{12}$ Ω cm at room temperature, which is higher by two orders of magnitude as compared to films deposited at 550 °C. The $C-V$ characteristics measured at frequency of 1 MHz for the MIMS capacitors are shown in Fig. 7. The capacitance of the STO film deposited at 550 °C is almost constant in the bias voltage ranging from −5 to 5 V. However, for the STO film deposited at 700 °C, the $C-V$ curve shows small variation in capacitance as a function of applied field. The field dependence of the dielectric constant is attributed to the nature, work function of the contact layers, and the interface states.[14–16] The relative dielectric constant estimated from the maximum value of capacitance was found to be 312 for the film grown at $T_s=700$ °C and 186 for the film grown at 550 °C, respectively. It should be noted that the dielectric constant of our epitaxial films on Si with TiN template is one of the highest values so far reported for the STO films grown on Si. The $C-V$ curves measured with increasing and decreasing bias voltage showed very small hysteresis in each curve. This indicates that the dielectric films have negligible ferroelectric effects and concomitant polarizable ion conduction. The higher values of resistivity, breakdown fields and high dielectric constant are attributed to excellent crystallinity of the perovskite STO films. These values are sufficiently high for dielectric applications of these heterostructures. For DRAM applications, one needs a film with high charge storage density and low leakage current density. Recently, Krupanidhi *et al.*[4] showed that the STO films had one order of magnitude higher capacitance density at relatively larger thicknesses compared to gate dielectrics such as SiO_2 and Ta_2O_5. In our films, the charge storage density was calculated from the relation $Q_c=\epsilon_0\epsilon_r E$, where E is the applied electric field, ϵ_0 is the dielectric constant of vacuum, and ϵ_r is the permittivity of the STO film. From our $C-V$ measurements, the Q_c was estimated to be 76.8 fC/μm^2 at an electric field of about 250 kV cm^{-1}. This

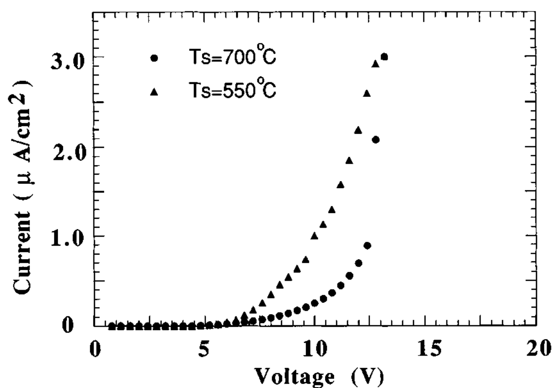

FIG. 6. Room-temperature $I-V$ characteristics of Au/STO/TiN/Si MIMS type heterostructures wherein the STO films were grown on epitaxial TiN/Si at substrate temperature (T_s) of 550 and 700 °C.

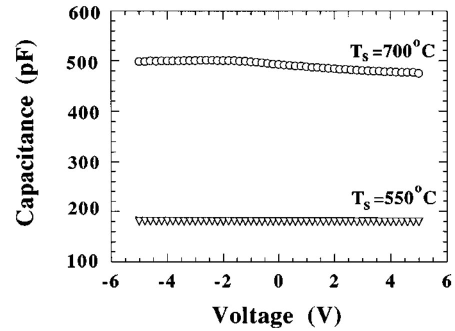

FIG. 7. Typical capacitance vs applied voltage curves measured at 1 MHz for the MIMS structures fabricated at 550 and 700 °C.

Downloaded¬15¬Nov¬2002¬to¬129.2.41.143.¬Redistribution¬subject¬to¬AIP¬license¬or¬copyright,¬see¬http://ojps.aip.org/japo/japcr.jsp

value appears to be consistent with that of reported for STO films.[4]

IV. CONCLUSION

In conclusion, we have fabricated high-quality ceramic based insulator/metal/Si, i.e., STO/TiN/Si(100) heterostructures by *in situ* PLD. It is found that the thin epitaxial TiN layer promotes high-quality epitaxial growth of STO perovskite on silicon. The XRD, RBS, and TEM results revealed that the STO films grow epitaxially on epi-TiN/Si(100) above 500 °C with epitaxial relationship as ⟨100⟩STO‖⟨100⟩TiN‖⟨100⟩Si, i.e., cube-on-cube epitaxy. The electrical properties of the MIM type capacitor structures were investigated. For a 1800 Å STO film grown on TiN/Si at $T_s = 700$ °C and O_2 partial pressure in the range of 1–10 mTorr, the dielectric constant was found to be 312 at 1 MHz. The electrical resistivity and breakdown field of the STO films were more than $\sim 5\times 10^{12}\ \Omega$ cm and $\sim 5\times 10^{5}$ V cm^{-1}, respectively. We anticipate that the epitaxial heterostructures on Si with TiN contact layer will provide significant improvement in advanced microelectronic devices.

[1] *Amorphous Insulating Thin Films II*, edited by R. A. B. Devine, W. L. Warren, J. Kanicki, and M. Matsumara (Elsevier, New York, 1995), and references therein.

[2] See, for example, in *Proceedings of the Materials Research Society Symposium on Ferroelectric Thin Films III*, edited by S. B. Desu, P. K. Larsen, E. R. Myers, and B. A. Tuttle (Material Research Society, Pittsburgh, 1993).

[3] P. C. Joshi and S. B. Krupanidhi, J. Appl. Phys. **73**, 7627 (1993).

[4] G. M. Rao and S. B. Krupanidhi, J. Appl. Phys. **75**, 2604 (1994); D. Roy, J. Peng, and S. B. Krupanidhi, Appl. Phys. Lett. **60**, 2478 (1992).

[5] B. K. Moon and H. Ishiwara, Jpn. J. Appl. Phys. 1 **33**, 1472 (1994); Jpn. J. Appl. Phys. 1 **33**, 5911 (1994); Appl. Phys. Lett. **67**, 1996 (1995).

[6] L. S. Hung, G. M. Mason, G. R. Paz-Pujalt, J. A. Agostinelli, J. M. Mir, S. T. Lee, T. N. Blanton, and G. Ding, J. Appl. Phys. **74**, 1366 (1993).

[7] T. Sakuma, S. Yamamichi, S. Matsubara, H. Yamaguchi, and Y. Miyasaka, Appl. Phys. Lett. **57**, 2431 (1990).

[8] H. Ishiwara, N. Tsuji, H. Mori, and H. Nohira, Appl. Phys. Lett. **61**, 1459 (1992).

[9] J. Narayan, P. Tiwari, X. Chen, J. Singh, R. Chowdhury, and T. Zheleva, Appl. Phys. Lett. **61**, 1290 (1990); U. S. Patent No. 5 406 123 (11 April 1995).

[10] R. D. Vispute, R. Chowdhury, P. Tiwari, and J. Narayan, Appl. Phys. Lett. **65**, 2565 (1994).

[11] M. Hiratani, Y. Tarutani, T. Fukazawa, M. Okamoto, and K. Takagi, Thin Solid Films **227**, 100 (1993).

[12] L. J. Schowalter, R. W. Fathauer, R. P. Goehner, L. G. Turner, R. W. DeBlois, S. Hashimoto, J.-L. Peng, W. M. Gibson, and J. P. Krusius, J. Appl. Phys. **58**, 302 (1985).

[13] Q. Li, O. Meyer, X. X. Xi, J. Geerk, and G. Linker, Appl. Phys. Lett. **55**, 310 (1989).

[14] K. Abe and S. Komatsu, Jpn. J. Appl. Phys. 1 **31**, 2985 (1992).

[15] M. Iwabuchi, K. Kinoshita, H. Ishibashi, and T. Kobayashi, Jpn. J. Appl. Phys. 1 **33**, L610 (1994).

[16] T. Hirano, M. Ueda, K. Matsui, T. Fujii, K. Sakuta, and T. Kobayashi, Jpn. J. Appl. Phys. 1 **31**, L1345 (1992).

Downloaded¬15¬Nov¬2002¬to¬129.2.41.143.¬Redistribution¬subject¬to¬AIP¬license¬or¬copyright,¬see¬http://ojps.aip.org/japo/japcr.jsp